

EliteKV: Scalable KV Cache Compression via RoPE Frequency Selection and Joint Low-Rank Projection

Yuhao Zhou*, Sirui Song*, Boyang Liu,
Zhiheng Xi, Senjie Jin, Xiaoran Fan, Zhihao Zhang, Wei Li, Xuanjing Huang[†]

Fudan University

{zhouyh24, srsong23}@m.fudan.edu.cn, xjhuang@fudan.edu.cn

Abstract

Rotary Position Embedding (RoPE) enables each attention head to capture multi-frequency information along the sequence dimension and is widely applied in foundation models. However, the nonlinearity introduced by RoPE complicates optimization of the key state in the Key-Value (KV) cache for RoPE-based attention. Existing KV cache compression methods typically store key state before rotation and apply the transformation during decoding, introducing additional computational overhead. This paper introduces *EliteKV*, a flexible modification framework for RoPE-based models supporting variable KV cache compression ratios. *EliteKV* first identifies the intrinsic frequency preference of each head using *RoPElite*, selectively restoring linearity to certain dimensions of key within attention computation. Building on this, joint low-rank compression of key and value enables partial cache sharing. Experimental results show that with minimal uptraining on only 0.6% of the original training data, RoPE-based models achieve a 75% reduction in KV cache size while preserving performance within a negligible margin. Furthermore, *EliteKV* consistently performs well across models of different scales within the same family.¹

1 Introduction

Large language foundation models demonstrates remarkable capabilities in solving a wide range of problems in the language domain (Jaech et al., 2024; Touvron et al., 2023; DeepSeek-AI et al., 2025). To accelerate inference, a simple yet effective technique is to cache the key and value (KV cache) in the attention mechanism (Vaswani et al., 2017) to avoid redundant computations. However, the size of the KV cache grows linearly

with the number of decoding steps (Pope et al., 2023; Fu, 2024), which becomes a limitation for real-world, long-text, and real-time applications (Li et al., 2024). Therefore, compressing the KV cache becomes a key issue for improving inference efficiency.

A mainstream approach to compressing the KV cache is to perform low-rank decomposition on the key and value projection matrices, which allows replacing the cached content with lower-dimensional intermediate states (Zhang et al., 2024a; Wang et al., 2025). However, with the widespread use of rotary position embedding (Su et al., 2024, RoPE), which have nonlinear properties, the application of such methods becomes challenging. The nonlinear nature of RoPE prevents caching the rotated intermediate states with lower dimensions, limiting the cache to storing the pre-rotated states (Chang et al., 2025). When applying RoPE again to all cache entries during usage, additional computation is introduced during decoding, which contradicts the original design intention of the KV cache (Zhang et al., 2024b; Sun et al., 2024; Chang et al., 2025).

This work describes *EliteKV*, a straightforward method that bypasses the constraints imposed by the non-linear nature of RoPE and allows for the compression of KV cache to any specified proportion of the original size. *EliteKV* aims to eliminate RoPE in certain dimensions of the attention computation flow, enabling the compression of the cache formed by those dimensions. Specifically, first, based on the varying frequency preferences of each attention head, the combination of dimensions in the rotation that each attention head relies on the most is identified. Then, a joint low-rank decomposition (J-LRD) is performed on the projection matrices of the parts of the key without RoPE and the entire value for all heads in the same layer, enabling them to be decomposed into a shared down-projection matrix and corresponding

* Equal contribution.

[†] Corresponding authors.

¹ Codes are publicly available at [CiaranZhou/EliteKV](https://github.com/CiaranZhou/EliteKV).

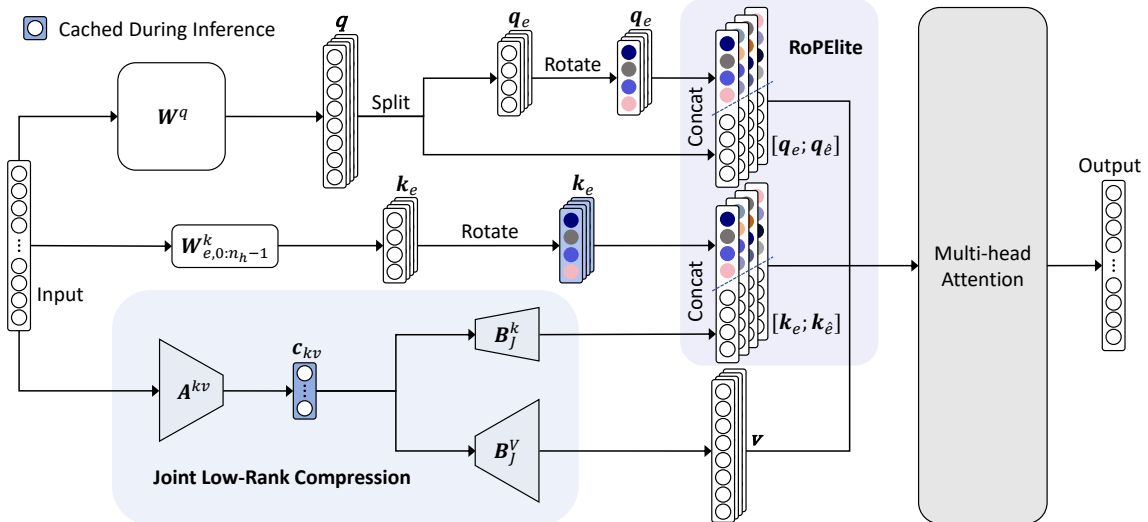


Figure 1: The attention computation flow after applying *EliteKV*. The upper part illustrates *RoPElite*, where each attention head focuses only on its most important frequency along the sequence dimension. The lower part shows the joint low-rank projection, where the K and V states are represented by a shared cache. The different colored fillings in the elements represent 2D chunks attending to different frequencies.

up-projection matrix. The resulting modified attention computation flow, as shown in Figure 1. Each head only selects the frequency information most relevant to it in the sequence dimension for RoPE which call *RoPElite*. Beyond that, the remaining parts of the key state without RoPE and the entire value state are represented by a shared low-dimensional intermediate state.

Experimental results demonstrate the superiority of *EliteKV* as a method that modifies the model structure to achieve KV cache compression. It enables reducing the KV cache to just 25% of the original size while maintaining comparable performance. Additionally, when the KV cache is reduced to 12.5%, the performance is on par with GQA at 50%. Ablation studies further validate the effectiveness of *RoPElite* in searching for the optimal rotation dimension combination for each attention head. Moreover, J-LRD outperforms traditional low-rank decomposition methods, which treat each weight matrix separately, in terms of KV cache size reduction. As the model parameters scale, *EliteKV* shows predictable performance loss across different model sizes within the same family, highlighting its scalability and efficiency in maintaining performance.

2 Background

2.1 Attention Mechanism and KV Cache

The attention mechanism is a core component of the Transformer model, which measures the

importance of different tokens, allowing the model to focus on different parts of the input sequence (Vaswani et al., 2017). Given an input $\mathbf{x}_t \in \mathbb{R}^d$ at time step t , it is projected onto query, key, and value for each attention head h using the weight matrices $\mathbf{W}^q, \mathbf{W}^k, \mathbf{W}^v \in \mathbb{R}^{d \times d_h}$ ², where d represents the embedding dimension of each token and d_h denotes the dimension of each attention head. The process is formulated as follows: $\mathbf{q}_t = \mathbf{x}_t \mathbf{W}^q, \mathbf{k}_t = \mathbf{x}_t \mathbf{W}^k$ and $\mathbf{v}_t = \mathbf{x}_t \mathbf{W}^v$. Then the attention mechanism is as follows:

$$\mathbf{K}_t = \sum_{j=1}^t \mathbf{k}_j, \quad \mathbf{V}_t = \sum_{j=1}^t \mathbf{v}_j, \quad \mathbf{s}_t = \mathbf{q}_t \mathbf{K}_t^\top,$$

$$\mathbf{p}_t = \text{Softmax} \left(\frac{\mathbf{s}_t}{\sqrt{d_h}} \right), \quad \mathbf{o}_t = \mathbf{p}_t \mathbf{V}_t.$$

The autoregressive nature of decoder-only models allows for the reuse of key-value pairs cached from previous tokens (KV cache), reducing the computational cost during token-by-token decoding. At each decoding step t , the \mathbf{K}_t and \mathbf{V}_t are obtained by concatenating the cached \mathbf{K}_{t-1} and \mathbf{V}_{t-1} with the newly computed \mathbf{k}_t and \mathbf{v}_t .

2.2 Rotary Position Embedding (RoPE)

RoPE (Su et al., 2024) is a widely used method for incorporating positional information into Transformer models. It divides the dimensions of the

²Processes refer to a single attention head unless stated otherwise, with the subscript h omitted for simplicity.

query and key for each attention head into several 2D pairs, with each pair capturing information at different frequencies θ along the sequence dimension, thereby enabling the attention scores to carry positional information as shown by:

$$\mathbf{s}_{m[n]} = \sum_{i \in \mathcal{I}} (\mathbf{q}_{m,i} \mathbf{R}(m\theta_i)) (\mathbf{k}_{n,i} \mathbf{R}(n\theta_i))^\top \quad (1a)$$

$$= \sum_{i \in \mathcal{I}} \mathbf{q}_{m,i} \mathbf{R}((m-n)\theta_i) \mathbf{k}_{n,i}^\top \quad (1b)$$

where \mathbf{R} is a 2D rotation matrix,

$$\mathcal{I} = \{[2i : 2i + 1] \mid i = 0, 1, 2, \dots, \frac{d_h}{2} - 1\}.$$

For RoPE-based models, at the t -th decoding step,

$$\sum_{i \in \mathcal{I}} \mathbf{k}_{t,i} \mathbf{R}(t\theta_i) + \mathbf{v}_t$$

are incorporated into the KV cache.

2.3 Singular Value Decomposition (SVD)

SVD is a method widely used for dimensionality reduction and matrix approximation. Given a matrix $\mathbf{M} \in \mathbb{R}^{m \times n}$, the SVD decomposes it as $\mathbf{U}\mathbf{\Sigma}\mathbf{V}^\top$, where $\mathbf{U} \in \mathbb{R}^{m \times m}$ and $\mathbf{V} \in \mathbb{R}^{n \times n}$ are orthogonal matrices, and $\mathbf{\Sigma} \in \mathbb{R}^{m \times n}$ is a diagonal matrix with non-negative elements arranged in descending order along the diagonal. Let $\mathbf{A} = \mathbf{U}$, and $\mathbf{B} = \mathbf{\Sigma}\mathbf{V}^\top$, then the optimal rank- r approximation of the matrix \mathbf{M} is $\mathbf{A}_{[:, :r]} \mathbf{B}_{[r, :]}$, which changes the storage requirement to $\frac{mr+rn}{mn}$ times the original.

3 Framework of *EliteKV*

3.1 *RoPElite*: Retain the Frequency Most Attended to by Each Attention Head

Although different heads follow the same set of frequencies to compute attention scores during the model structure design phase (Dubey et al., 2024; Yang et al., 2024; DeepSeek-AI et al., 2024b), some prior works observe that different attention heads exhibit varying sensitivity to different frequency information when computing attention scores (Hong et al., 2024; Barbero et al., 2025), implying that the chunks in \mathcal{I} have different impacts on \mathbf{s} . We refer to the most influential chunks as *elite chunks*, and the top- r chunks formed by these *elite chunks* are denoted as \mathcal{I}_r^e .

Finding \mathcal{I}_r^e for each attention head is challenging, as there are $\binom{\frac{d_h}{2}}{r}$ ways to choose r elements from \mathcal{I} ,

Algorithm 1 *RoPElite*

Require: head dimension d_h , collection of Rope pairs \mathcal{I} , number of elite chunks r

Ensure: elite chunks e

Initialize $e \leftarrow \emptyset$ as an empty list

for $i = 1$ to r **do**

$\hat{\mathbf{q}}_t, \hat{\mathbf{K}}_t \leftarrow \text{Apply RoPE}(\mathbf{q}_t, \mathbf{K}_t, \mathcal{I})$

$\mathbf{s} \leftarrow \text{attn_score}(\hat{\mathbf{q}}_t, \hat{\mathbf{K}}_t)$

$\mathbf{q}_t, \mathbf{K}_t \leftarrow \text{Apply RoPE}(\mathbf{q}_t, \mathbf{K}_t, \mathcal{I}_{i-1}^e)$

for j in \mathcal{I}_{i-1}^e **do**

$\mathbf{q}'_t, \mathbf{K}'_t \leftarrow \text{Apply RoPE}(\mathbf{q}_t, \mathbf{K}_t, j)$

$\mathbf{s}' \leftarrow \text{attn_score}(\mathbf{q}'_t, \mathbf{K}'_t)$

$\text{distance}[j] \leftarrow \|\mathbf{s} - \mathbf{s}'\|_1$

end for

$j^* \leftarrow \arg \min(\text{distance})$

Append j^* to e

end for

return e

and the model has l layers with n_h heads per layer. Based on this, we propose *RoPElite*, which uses a greedy algorithm to find \mathcal{I}_r^e for each attention head, as shown in Algorithm 1. It fully leverages parallelism, enabling the traversal of l layers and n_h heads in a single forward pass, reducing the time complexity to $O(rh_d)$, independent of l and n_h (detailed analysis in Appendix B).

As an example, for the model LLaMA2-7B, where each head is trained on \mathcal{I} , the \mathcal{I}_8^e distributions across different layers and heads are visualized in Figure 2 (more detailed plots are in Appendix A, Figure 8). It is clear that different attention heads focus on different frequency patterns across the sequence dimension. Taking \mathcal{I}_8^e as an example, the frequency dependencies of attention heads can be categorized as follows (L for layer and H for head): primarily high-frequency (L0H22, L0H31), primarily low-frequency (L0H8, L23H8, L31H22), mixed extreme frequencies (L0H0, L0H26), and predominantly mid-frequency (most heads). Notably, high-frequency information is predominantly captured by heads in shallow layers.

After applying *RoPElite*, the calculation process of the attention scores changes from the Equation 1b to

$$\mathbf{s}_{m[n]} = \sum_{i \in \mathcal{I}_r^e} \mathbf{q}_{m,i} \mathbf{R}((m-n)\theta_i) \mathbf{k}_{n,i}^\top + \sum_{i \in \mathcal{I} \setminus \mathcal{I}_r^e} \mathbf{q}_{m,i} \mathbf{k}_{n,i}^\top.$$

Such modifications inevitably require uptraining the model. For different \mathcal{I}_r^e , the model’s perfor-

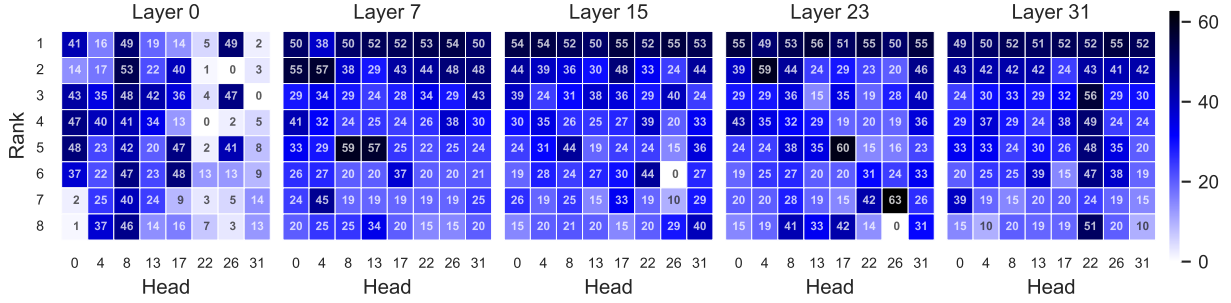


Figure 2: Top-8 chunks of different attention heads in different layers. Frequency preference patterns of different attention heads across layers in the LLaMA2-7B model. Numbers increase from high to low frequencies.

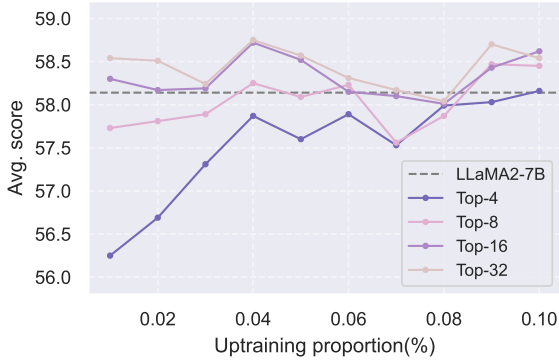


Figure 3: Performance of top- r chunks. **Uptraining proportion** represents the proportion of tokens relative to the total number of tokens used during training the original model.

mance varies with training, as shown in Figure 3. It can be observed that using only a small proportion of tokens, relative to the model’s original training tokens, during the uptraining phase can restore or even surpass the original performance. This suggests that retaining only the dimensions of high importance at the head level in a fully RoPE-trained model can maintain near full-frequency performance at the model level. A similar phenomenon was also observed by Lu et al. (2024). This implies that dimensions with lower importance may act as Gaussian noise in the calculation of attention scores.

For *RoPElite*-based models, at the t -th decoding step,

$$\sum_{i \in \mathcal{I}_r^e} \mathbf{k}_{t,i} \mathbf{R}(t\theta_i) + \sum_{i \in \mathcal{I} \setminus \mathcal{I}_r^e} \mathbf{k}_{t,i} + \mathbf{v}_t$$

are incorporated into the KV cache, which is consistent in size with that of RoPE-based models. The detailed workflow of *RoPElite* in the attention mechanism is shown on the upper part of Figure 1.

3.2 Low-Rank Compression for KV Cache

Optimizing the KV cache by low-rank decomposition of \mathbf{W}^k and \mathbf{W}^v in RoPE-based models is challenging. RoPE employs absolute position encoding (Equation 1a) to achieve relative position encoding (Equation 1b), which requires each head’s K cache to store $d_h = |\mathcal{I}| \times 2$ elements per token, otherwise additional computation is needed during decoding (see Section 5). The use of *RoPElite* alleviates this constraint by enabling partial compression of \mathbf{k} , bypassing the difficult-to-handle part of the RoPE cache and allowing the optimization of the KV cache size through $\sum_{i \in \mathcal{I} \setminus \mathcal{I}_r^e} \mathbf{k}_{t,i}$ and \mathbf{v}_t .

Let $\mathbf{W}_{e,h}^k \in \mathbb{R}^{d \times (2r)}$ denotes the portion of the key projection matrix for each attention head h that is responsible for \mathcal{I}_r^e , while $\mathbf{W}_{\hat{e},h}^k \in \mathbb{R}^{d \times (d_h - 2r)}$ represents the remaining part. To fully leverage the shared information across multiple heads, we consider performing low-rank decomposition on the projection matrix formed by all attention heads, rather than decomposing it on a per-head basis. Specifically, we handle the following combined projection matrices:

$$\begin{aligned} \mathbf{W}_{\hat{e},0:n_h-1}^k &= [\mathbf{W}_{\hat{e},0}^k, \mathbf{W}_{\hat{e},1}^k \cdots \mathbf{W}_{\hat{e},n_h-1}^k], \\ \mathbf{W}_{0:n_h-1}^v &= [\mathbf{W}_0^v, \mathbf{W}_1^v \cdots \mathbf{W}_{n_h-1}^v]. \end{aligned} \quad (2)$$

Depending on whether the K and V caches are optimized together, we explore *separated low-rank decomposition (S-LRD)* and *joint low-rank decomposition (J-LRD)*.

Separated Low-Rank Decomposition It is common to apply SVD for low-rank factorization of each weight matrix in the model (Zhang et al., 2024b; Chang et al., 2025; Wang et al., 2025), as it effectively reduces the model’s storage cost and the intermediate dimensionality. S-LRD allows for the customization of rank selection for each matrix,

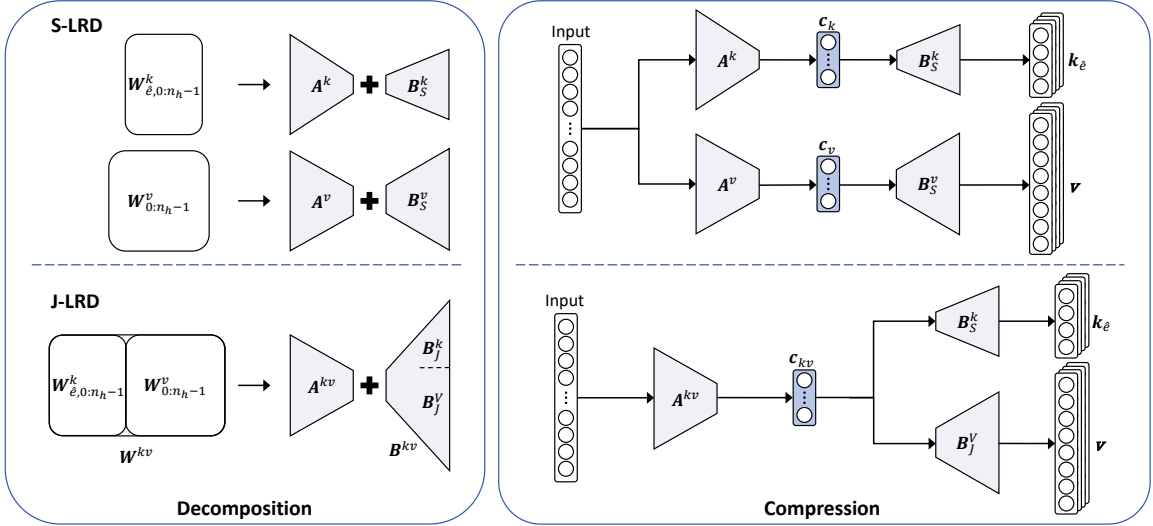


Figure 4: The projection matrices processed using S-LRD and J-LRD (Left), and the roles of the resulting matrices in the attention computation flow (Right).

leading to more precise approximations, which in turn minimizes performance degradation. S-LRD approximates the two matrices separately as:

$$\mathbf{W}_{\hat{e},0:n_h-1}^k \approx \mathbf{A}^k \mathbf{B}_S^k, \quad \mathbf{W}_{0:n_h-1}^v \approx \mathbf{A}^v \mathbf{B}_S^v,$$

where

$$\begin{aligned} \mathbf{A}^k &\in \mathbb{R}^{d \times d_{c_k}}, & \mathbf{B}_S^k &\in \mathbb{R}^{d_{c_k} \times (d_h n_h - 2rn_h)}, \\ \mathbf{A}^v &\in \mathbb{R}^{d \times d_{c_v}}, & \mathbf{B}_S^v &\in \mathbb{R}^{d_{c_v} \times (d_h n_h)}. \end{aligned}$$

The storage cost of *RoPElite* with S-LRD is given by:

$$2rn_h d + d_{c_k}(d + d_h n_h - 2rn_h) + d_{c_v}(d + d_h n_h),$$

which simplifies to:

$$(2d_{c_k} + 2d_{c_v} + 2rn_h)d - 2d_{c_k}rn_h,$$

in the case of MHA models, where the structural design typically follows $d = d_h n_h$. The KV cache consumption per token per layer is $2rn_h + d_{c_k} + d_{c_v}$.

Joint Low-Rank Decomposition From the perspective of sharing the KV cache, we propose J-LRD, which performs low-rank decomposition while simultaneously considering both K and V, leveraging the shared information between the two projection matrices. In J-LRD, the concatenated weight matrices are factorized as

$$\mathbf{W}^{kv} = \left[\mathbf{W}_{\hat{e},0:n_h-1}^k, \mathbf{W}_{0:n_h-1}^v \right] \approx \mathbf{A}^{kv} \mathbf{B}^{kv},$$

where

$$\mathbf{A}^{kv} \in \mathbb{R}^{d \times d_{c_{kv}}}, \quad \mathbf{B}^{kv} \in \mathbb{R}^{d_{c_{kv}} \times (2d_h n_h - 2rn_h)}.$$

The matrix used for up-projection is then split into:

$$\mathbf{B}^{kv} = [\mathbf{B}_J^k, \mathbf{B}_J^v],$$

where

$$\mathbf{B}_J^k \in \mathbb{R}^{d_{c_{kv}} \times (d_h n_h - 2rn_h)}, \quad \mathbf{B}_J^v \in \mathbb{R}^{d_{c_{kv}} \times (d_h n_h)}.$$

Under this factorization, the storage cost of *RoPElite* with J-LRD is expressed as:

$$2rn_h d + d_{c_{kv}}(d + 2d_h n_h - 2rn_h).$$

By simplifying the expression under the common MHA assumption, this reduces to:

$$2rn_h d + 3d_{c_{kv}}d - 2d_{c_{kv}}rn_h.$$

Furthermore, the KV cache requirement per token per layer in this setting is $2rn_h + d_{c_{kv}}$.

The workflows of S-LRD and J-LRD are shown in Figure 4, with the matrix decomposition process depicted on the left side of the figure, and the role of the resulting matrices in the new attention computation flow shown on the right side. J-LRD is chosen as the final component, and a detailed analysis of the experiments is provided in Section 4.3.2.

Finally, the framework of *RoPElite* with J-LRD is illustrated in Figure 1. From the perspective of KV cache, the approach first eliminates less critical RoPE dimensions in the original model, creating space for the remaining KV cache components to be projected into a low-rank latent space. Notably, this eliminates the need to reapply the rotation to

the keys in the cache during each decoding step. Next, leveraging the shared information between key and value, the projection matrices of both are jointly decomposed, enabling key-value pairs to be stored in a shared cache. This design is both parameter-efficient and KV cache-efficient. Finally, the optimal dimension configurations are selected based on simple filtering principles. The model is then uptrained from its unmodified state using the selected dimensions, resulting in a KV cache-efficient model.

4 Experiments

4.1 Benchmarks and Training Details

Models and Datasets. We conducted the primary experiments on the widely used open-source LLaMA2-7B (Touvron et al., 2023) model, and scaling experiments at the model size level on the LLaMA2-13B model. The pretraining data, RefinedWeb (Penedo et al., 2023), is open-source and of comparable quality to the original LLaMA2 pretraining data (something not achievable by the newer models), which is also the source of all the training data we used.

Perplexity Evaluation. We extracted a portion of the data from RefinedWeb as a holdout dataset to calculate the language perplexity of the model.

Benchmarks. To comprehensively evaluate the capabilities of the model, we assess its ability in commonsense reasoning, world knowledge, reading comprehension, and math reasoning. Specifically, we employ lm-evaluation-harness (Gao et al., 2024) to assess its performance on 8 tasks, including BoolQ (Clark et al., 2019), HellaSwag (Zellers et al., 2019), OpenBookQA (Mihaylov et al., 2018), Winogrande (Sakaguchi et al., 2021), GSM8K (Cobbe et al., 2021), TriviaQA (Joshi et al., 2017), ARC easy and challenge (Clark et al., 2018). All tasks are evaluated under the zero-shot setting, except for GSM8K (8-shot) and TriviaQA (5-shot).

Training Details. All models are trained with AdamW optimizer (Loshchilov and Hutter, 2019), with $\beta = [0.9, 0.95]$ and weight decay of 0.1. We employ a constant learning rate, which is set to the minimum learning rate at the end of the model’s pretraining phase. All training was conducted on the NVIDIA H100 platform, using ZeRO-2 (Rajbhandari et al., 2020) for memory management. Each training step includes 512 sequences, each with a length of 4096 tokens.

4.2 Experimental Result

We performed uptraining on the model with multiple target KV cache sizes, using less than 0.6% of the tokens from the model’s original pretraining phase. We compare *EliteKV* with GQA (Ainslie et al., 2023), a method that modifies the model structure to benefit from optimizations in the KV cache. The performance results on several benchmarks are shown in Table 1. *EliteKV* outperforms across all tested KV cache ratios. As the KV cache size decreases, the slower performance degradation allows *EliteKV* to retain performance comparable to the original model even when the KV cache is reduced to 25%. Additionally, thanks to the flexibility of the *RoPElite* and J-LRD dimension combinations, *EliteKV* is able to adjust the target KV cache ratio with finer granularity.

4.3 Analysis and Discussion

4.3.1 Retention of Rotated Dimensions

It is essential to determine that trained RoPE-based models exhibit frequency preference differences at the head level. To address this, we designed a method that uniformly retains a specified number of rotated dimensions across frequencies, which called *Uniform*. Also, it is crucial to demonstrate the superiority of *RoPElite* over other methods that determine rotated dimensions at the head level. We use the L2 norm of the RoPE chunks corresponding to each frequency as a measure of the contribution of each frequency’s corresponding dimension to the attention score. This measure is referred to as *Contribution* (Hong et al., 2024; Barbero et al., 2025).

We reduce the number of RoPE chunks in the model to a specified proportion using the two methods outlined above, as well as *RoPElite*. The proportions tested ranged from 1/2 to 1/16. The model was then uptrained using less than 0.1% of the original model’s pretraining tokens. As shown in Table 2, *Uniform* performs similarly to other methods at higher proportions. However, as the proportion decreases, the performance gap between it and the others that customize dimensions per head becomes increasingly apparent. Across all tested proportions, *RoPElite* consistently outperforms the other approaches, with the performance difference becoming more pronounced at lower proportions. This further confirms the importance of identifying a dedicated frequency preference pattern for each attention head and demonstrates the effectiveness

Cache	Method	Arc-C	Arc-E	BoolQ	HS	OB	WG	GSM	TQA	Avg.(6)	Avg.(8)
100.0	LLaMA2-7B	46.08	74.54	77.77	75.84	44.00	68.75	14.18	63.99	64.50	58.14
50.0	GQA	43.94	72.47	73.98	73.76	41.60	68.43	8.04	60.39	62.36	55.33
	<i>EliteKV</i>	47.10	74.92	75.63	75.66	44.00	69.22	11.22	64.02	64.42	57.72
34.4	<i>EliteKV</i>	46.33	74.75	77.03	75.51	43.40	69.06	11.75	63.38	64.33	57.65
28.1	<i>EliteKV</i>	45.99	74.28	77.25	75.38	44.40	69.53	11.83	63.05	64.47	57.71
25.0	GQA	40.78	70.37	72.23	71.81	40.80	66.14	3.11	55.51	60.36	52.59
	<i>EliteKV</i>	44.88	74.49	76.51	75.21	43.20	69.06	12.51	62.51	63.89	57.30
21.9	<i>EliteKV</i>	44.11	73.40	74.86	74.94	43.00	68.82	10.39	62.00	63.19	56.44
12.5	GQA	40.10	69.11	68.26	69.84	39.80	62.83	2.05	50.49	58.32	50.31
	<i>EliteKV</i>	44.20	73.99	74.46	74.40	41.40	67.56	9.40	59.94	62.67	55.67

Table 1: The scores of *EliteKV* and GQA on 8 benchmarks. Avg.(6) for the first 6 and Avg.(8) represents all. **Cache** represents the proportion of the current KV cache relative to that of the original model.

Method	$r = 32$	$r = 16$	$r = 8$	$r = 4$
<i>Uniform</i>	58.33	58.11	57.69	57.49
<i>Contribution</i>	58.24	58.30	58.00	57.84
<i>RoPElite</i>	58.54	58.62	58.45	58.16

Table 2: Average scores of different rotation dimension search methods across 8 benchmarks. r represents the number of 2D chunks assigned to each attention head, responsible for a specific frequency. When $r = 64$, corresponding to the original model, the performance is 58.14.

of the *RoPElite* in the search for optimal rotated dimensions.

4.3.2 Low-Rank Decomposition

Section 3.2 provides an analysis of the parameter count and KV cache size for both S-LRD and J-LRD. It is evident that, for the same parameter constraints, J-LRD results in a smaller KV cache size compared to S-LRD. Additionally, we used a greedy algorithm to find the optimal combination of d_{c_k} and d_{c_v} for S-LRD, given the KV cache size for each layer of attention. We then evaluate the language perplexity of both methods using the models trained in Section 4.3.1.

As shown in Figure 5, in multiple settings, even though S-LRD has the advantage of customizability, it fails to outperform J-LRD when the KV cache size is fixed. This confirms the forward-looking nature of J-LRD, which leverages shared information between K and V.

4.3.3 Impact of Training Token Quantity on Model Performance Recovery

Since this method inevitably requires uptraining, a key concern is the speed at which model performance recovers at different KV cache ratios. As shown in Figure 6, for higher KV cache

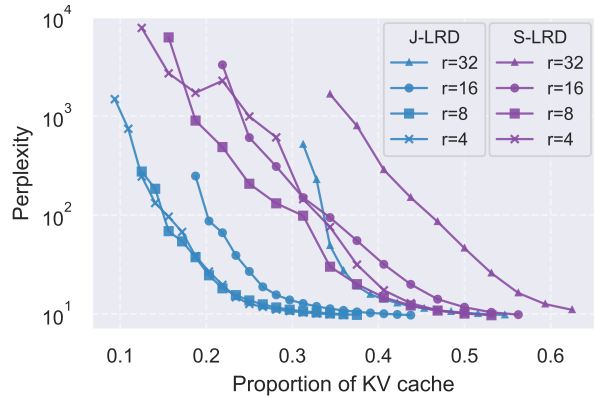


Figure 5: The perplexity of the *RoPElite* model on the dataset with varying compression ratios of the KV cache, as the number of frequency-related chunks retained for each attention head changes under S-LRD and J-LRD. Only points without additional parameter overhead are shown.

sizes, the model performance converges quickly. However, for lower ratios, such as 12.5%, more training effort is required. Therefore, when aiming for a model with a KV cache size smaller than 25% of the original, one must choose the cache size based on the acceptable training cost, or combine it with other techniques to reduce KV cache size, such as quantization (Zhao et al., 2024; Hooper et al., 2024; Liu et al., 2024).

4.3.4 Performance Differences Across Model Sizes

In general, larger models have more attention heads, which means that when the same number of chunks is retained for each head, the multi-head attention mechanism aggregates more positional information. Additionally, larger weight matrices may also contain more redundant information. We explored the larger LLaMA2-13B model and used the percentage of performance loss during training

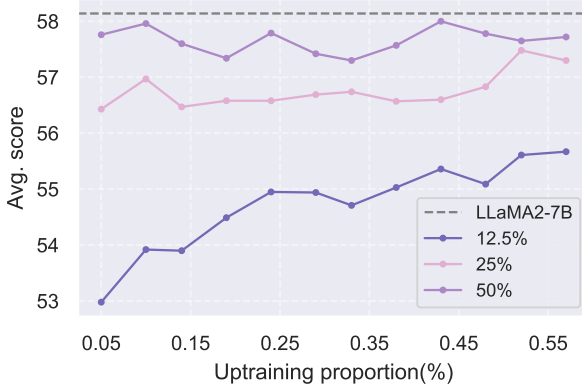


Figure 6: The performance trend of the model after applying *EliteKV*, as training progresses, under varying KV cache compression ratios.

as an observation point for training dynamics. As shown in Figure 7, when upraining the same number of tokens, larger models exhibit faster convergence. The relative performance loss across models of different scales reaches a similar upper bound, suggesting that the performance loss due to convergence limits is consistent across model sizes.

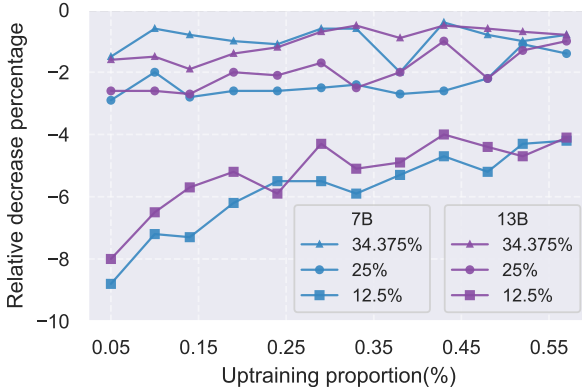


Figure 7: The relative percentage decrease in average scores across 8 benchmarks for LLaMA2 family models (7B and 13B) after applying *EliteKV*, under different KV cache compression ratios.

5 Related Work

SVD for KV Cache Compression Many works have focused on performing low-rank decomposition of the key and value projection matrices into $\mathbf{A}^k \mathbf{B}^k$ and $\mathbf{A}^v \mathbf{B}^v$ (Zhang et al., 2024b; Sun et al., 2024; Chang et al., 2025). Like these methods, our approach also reduces the intermediate tensor dimensions by absorbing \mathbf{B}^k and \mathbf{B}^v into the rest of the matrix computations to cache lower-dimensional intermediate tensors (DeepSeek-AI

et al., 2024a,b). However, because of the non-linear nature of positional embeddings, these methods can only cache $\mathbf{x}\mathbf{A}^k$ and $\mathbf{x}\mathbf{A}^v$ as the new KV cache. This requires designing specialized GPU kernels to reconstruct the rotation process of the keys at each decoding step. Thanks to *RoPElite*, our approach achieves KV cache efficiency not by handling the non-linear components but by leveraging the remaining linear parts.

Efficient MHA Variants for KV Cache Several notable efforts have aimed at reducing the use of KV cache through the redesign of multi-head attention mechanisms. GQA (Ainslie et al., 2023) and MQA (Shazeer, 2019) (GQA with group size 1) focus on reducing the number of K and V heads. MLA (DeepSeek-AI et al., 2024a,b) and MFA (Hu et al., 2024) aim to project K and V into a lower-rank space. In contrast to our approach, which operates on pretrained models, these methods are applied at the model design stage before pretraining, with only GQA allowing modifications based on an already trained model. Our method, by principle, can be applied to both pretrained MHA-based models and QGA-based models, and the modified attention structure can also inform future model design.

6 Conclusion

We propose *EliteKV* for reducing the KV cache size in RoPE-based models with high flexibility, composed of two main components. First, *RoPElite* identifies the varying frequency preferences across different attention heads in RoPE-based models, demonstrating that, after a small amount of upraining, retaining only the most important dimensions of RoPE still allows the model to recover its original performance. This enables subsequent low-rank compression of the KV cache to avoid dealing with the non-linear components of RoPE. Second, for the compression part, J-LRD takes into account the shared information between the K and V projection matrices during their decomposition. This allows the KV cache to be further reduced compared to traditional methods that treat the projection matrices separately. Experimental results show that, compared to GQA, *EliteKV* recovers performance similar to the original model more quickly under higher KV cache settings. In lower KV cache settings, the relative performance loss is less than 1/3 of that observed in the baseline.

Limitations

Since pretrained models with publicly available datasets are becoming increasingly rare, and as the number of tokens used in the pretraining phase of base models grows (e.g., 15T for LLaMA3), foundation models are becoming increasingly well-trained. This leads to a higher demand for tokens during modifications to restore model performance. Therefore, the models explored in this paper are limited.

References

- Joshua Ainslie, James Lee-Thorp, Michiel de Jong, Yury Zemlyanskiy, Federico Lebron, and Sumit Sanghai. 2023. [GQA: Training generalized multi-query transformer models from multi-head checkpoints](#). In *Proceedings of the 2023 Conference on Empirical Methods in Natural Language Processing*, pages 4895–4901, Singapore. Association for Computational Linguistics.
- Federico Barbero, Alex Vitvitskiy, Christos Perivolaropoulos, Razvan Pascanu, and Petar Veličković. 2025. [Round and round we go! what makes rotary positional encodings useful?](#) In *The Thirteenth International Conference on Learning Representations*.
- Chi-Chih Chang, Wei-Cheng Lin, Chien-Yu Lin, Chong-Yan Chen, Yu-Fang Hu, Pei-Shuo Wang, Ning-Chi Huang, Luis Ceze, Mohamed S. Abdelfattah, and Kai-Chiang Wu. 2025. [Palu: KV-cache compression with low-rank projection](#). In *The Thirteenth International Conference on Learning Representations*.
- Christopher Clark, Kenton Lee, Ming-Wei Chang, Tom Kwiatkowski, Michael Collins, and Kristina Toutanova. 2019. [BoolQ: Exploring the surprising difficulty of natural yes/no questions](#). In *Proceedings of the 2019 Conference of the North American Chapter of the Association for Computational Linguistics: Human Language Technologies, Volume 1 (Long and Short Papers)*, pages 2924–2936, Minneapolis, Minnesota. Association for Computational Linguistics.
- Peter Clark, Isaac Cowhey, Oren Etzioni, Tushar Khot, Ashish Sabharwal, Carissa Schoenick, and Oyvind Tafjord. 2018. [Think you have solved question answering? try arc, the AI2 reasoning challenge](#). *CoRR*, abs/1803.05457.
- Karl Cobbe, Vineet Kosaraju, Mohammad Bavarian, Mark Chen, Heewoo Jun, Lukasz Kaiser, Matthias Plappert, Jerry Tworek, Jacob Hilton, Reiichiro Nakano, Christopher Hesse, and John Schulman. 2021. [Training verifiers to solve math word problems](#). *CoRR*, abs/2110.14168.
- DeepSeek-AI, Daya Guo, Dejian Yang, Haowei Zhang, Junxiao Song, Ruoyu Zhang, Runxin Xu, Qihao Zhu, Shirong Ma, Peiyi Wang, Xiao Bi, Xiaokang Zhang, Xingkai Yu, Yu Wu, Z. F. Wu, Zhibin Gou, Zhihong Shao, Zhuoshu Li, Ziyi Gao, Aixin Liu, Bing Xue, Bingxuan Wang, Bochao Wu, Bei Feng, Chengda Lu, Chenggang Zhao, Chengqi Deng, Chenyu Zhang, Chong Ruan, Damai Dai, Deli Chen, Dongjie Ji, Erhang Li, Fangyun Lin, Fucong Dai, Fuli Luo, Guangbo Hao, Guanting Chen, Guowei Li, H. Zhang, Han Bao, Hanwei Xu, Haocheng Wang, Honghui Ding, Huajian Xin, Huazuo Gao, Hui Qu, Hui Li, Jianzhong Guo, Jiashi Li, Jiawei Wang, Jingchang Chen, Jingyang Yuan, Junjie Qiu, Junlong Li, J. L. Cai, Jiaqi Ni, Jian Liang, Jin Chen, Kai Dong, Kai Hu, Kaige Gao, Kang Guan, Kexin Huang, Kuai Yu, Lean Wang, Lecong Zhang, Liang Zhao, Litong Wang, Liyue Zhang, Lei Xu, Leyi Xia, Mingchuan Zhang, Minghua Zhang, Minghui Tang, Meng Li, Miaojun Wang, Mingming Li, Ning Tian, Panpan Huang, Peng Zhang, Qiancheng Wang, Qinyu Chen, Qiushi Du, Ruiqi Ge, Ruisong Zhang, Ruizhe Pan, Runji Wang, R. J. Chen, R. L. Jin, Ruyi Chen, Shanghao Lu, Shangyan Zhou, Shanhuang Chen, Shengfeng Ye, Shiyu Wang, Shuiping Yu, Shunfeng Zhou, Shuting Pan, S. S. Li, Shuang Zhou, Shaoqing Wu, Shengfeng Ye, Tao Yun, Tian Pei, Tianyu Sun, T. Wang, Wangding Zeng, Wanbiao Zhao, Wen Liu, Wenfeng Liang, Wenjun Gao, Wenqin Yu, Wentao Zhang, W. L. Xiao, Wei An, Xiaodong Liu, Xiaohan Wang, Xiaokang Chen, Xiaotao Nie, Xin Cheng, Xin Liu, Xin Xie, Xingchao Liu, Xinyu Yang, Xinyuan Li, Xuecheng Su, Xuheng Lin, X. Q. Li, Xiangyue Jin, Xiaojin Shen, Xiaosha Chen, Xiaowen Sun, Xiaoxiang Wang, Xinnan Song, Xinyi Zhou, Xianzu Wang, Xinxia Shan, Y. K. Li, Y. Q. Wang, Y. X. Wei, Yang Zhang, Yanhong Xu, Yao Li, Yao Zhao, Yaofeng Sun, Yaohui Wang, Yi Yu, Yichao Zhang, Yifan Shi, Yiliang Xiong, Ying He, Yishi Piao, Yisong Wang, Yixuan Tan, Yiyang Ma, Yiyuan Liu, Yongqiang Guo, Yuan Ou, Yudian Wang, Yue Gong, Yuheng Zou, Yujia He, Yunfan Xiong, Yuxiang Luo, Yuxiang You, Yuxuan Liu, Yuyang Zhou, Y. X. Zhu, Yanhong Xu, Yanping Huang, Yaohui Li, Yi Zheng, Yuchen Zhu, Yunxian Ma, Ying Tang, Yukun Zha, Yuting Yan, Z. Z. Ren, Zehui Ren, Zhangli Sha, Zhe Fu, Zhean Xu, Zhenda Xie, Zhengyan Zhang, Zhewen Hao, Zhicheng Ma, Zhigang Yan, Zhiyu Wu, Zihui Gu, Zijia Zhu, Zijun Liu, Zilin Li, Ziwei Xie, Ziyang Song, Zizheng Pan, Zhen Huang, Zhipeng Xu, Zhongyu Zhang, and Zhen Zhang. 2025. [Deepseek-r1: Incentivizing reasoning capability in llms via reinforcement learning](#). *CoRR*, abs/2501.12948.
- DeepSeek-AI, Aixin Liu, Bei Feng, Bin Wang, Bingxuan Wang, Bo Liu, Chenggang Zhao, Chengqi Deng, Chong Ruan, Damai Dai, Daya Guo, Dejian Yang, Deli Chen, Dongjie Ji, Erhang Li, Fangyun Lin, Fuli Luo, Guangbo Hao, Guanting Chen, Guowei Li, Hao Zhang, Hanwei Xu, Hao Yang, Haowei Zhang, Honghui Ding, Huajian Xin, Huazuo Gao, Hui Li, Hui Qu, J. L. Cai, Jian Liang, Jianzhong Guo, Jiaqi Ni, Jiashi Li, Jin Chen, Jingyang Yuan, Junjie Qiu, Junxiao Song, Kai Dong, Kaige Gao, Kang Guan, Lean Wang, Lecong Zhang, Lei Xu, Leyi Xia, Liang Zhao, Liyue Zhang, Meng Li, Miaojun

- Wang, Mingchuan Zhang, Minghua Zhang, Minghui Tang, Mingming Li, Ning Tian, Panpan Huang, Peiyi Wang, Peng Zhang, Qihao Zhu, Qinyu Chen, Qiushi Du, R. J. Chen, R. L. Jin, Ruiqi Ge, Ruizhe Pan, Runxin Xu, Ruyi Chen, S. S. Li, Shanghao Lu, Shangyan Zhou, Shanhuang Chen, Shaoqing Wu, Shengfeng Ye, Shirong Ma, Shiyu Wang, Shuang Zhou, Shuiping Yu, Shunfeng Zhou, Size Zheng, Tao Wang, Tian Pei, Tian Yuan, Tianyu Sun, W. L. Xiao, Wangding Zeng, Wei An, Wen Liu, Wenfeng Liang, Wenjun Gao, Wentao Zhang, X. Q. Li, Xiangyue Jin, Xianzu Wang, Xiao Bi, Xiaodong Liu, Xiaohan Wang, Xiaojin Shen, Xiaokang Chen, Xiaosha Chen, Xiaotao Nie, and Xiaowen Sun. 2024a. [Deepseek-v2: A strong, economical, and efficient mixture-of-experts language model](#). *CoRR*, abs/2405.04434.
- DeepSeek-AI, Aixin Liu, Bei Feng, Bing Xue, Bingxuan Wang, Bochao Wu, Chengda Lu, Chenggang Zhao, Chengqi Deng, Chenyu Zhang, Chong Ruan, Damai Dai, Daya Guo, Dejian Yang, Deli Chen, Dongjie Ji, Erhang Li, Fangyun Lin, Fucong Dai, Fuli Luo, Guangbo Hao, Guanting Chen, Guowei Li, H. Zhang, Han Bao, Hanwei Xu, Haocheng Wang, Haowei Zhang, Honghui Ding, Huajian Xin, Huazuo Gao, Hui Li, Hui Qu, J. L. Cai, Jian Liang, Jianzhong Guo, Jiaqi Ni, Jiashi Li, Jiawei Wang, Jin Chen, Jingchang Chen, Jingyang Yuan, Junjie Qiu, Junlong Li, Junxiao Song, Kai Dong, Kai Hu, Kaige Gao, Kang Guan, Kexin Huang, Kuai Yu, Lean Wang, Lecong Zhang, Lei Xu, Leyi Xia, Liang Zhao, Litong Wang, Liyue Zhang, Meng Li, Miaojuan Wang, Mingchuan Zhang, Minghua Zhang, Minghui Tang, Mingming Li, Ning Tian, Panpan Huang, Peiyi Wang, Peng Zhang, Qiancheng Wang, Qihao Zhu, Qinyu Chen, Qiushi Du, R. J. Chen, R. L. Jin, Ruiqi Ge, Ruisong Zhang, Ruizhe Pan, Runji Wang, Runxin Xu, Ruoyu Zhang, Ruyi Chen, S. S. Li, Shanghao Lu, Shangyan Zhou, Shanhuang Chen, Shaoqing Wu, Shengfeng Ye, Shengfeng Ye, Shirong Ma, Shiyu Wang, Shuang Zhou, Shuiping Yu, Shunfeng Zhou, Shutong Pan, T. Wang, Tao Yun, Tian Pei, Tianyu Sun, W. L. Xiao, and Wangding Zeng. 2024b. [Deepseek-v3 technical report](#). *CoRR*, abs/2412.19437.
- Abhimanyu Dubey, Abhinav Jauhri, Abhinav Pandey, Abhishek Kadian, Ahmad Al-Dahle, Aiesha Letman, Akhil Mathur, Alan Schelten, Amy Yang, Angela Fan, Anirudh Goyal, Anthony Hartshorn, Aobo Yang, Archi Mitra, Archie Sravankumar, Artem Korenev, Arthur Hinsvark, Arun Rao, Aston Zhang, Aurélien Rodriguez, Austen Gregerson, Ava Spataru, Baptiste Rozière, Bethany Biron, Binh Tang, Bobbie Chern, Charlotte Caucheteux, Chaya Nayak, Chloe Bi, Chris Marra, Chris McConnell, Christian Keller, Christophe Touret, Chunyang Wu, Corinne Wong, Cristian Canton Ferrer, Cyrus Nikolaidis, Damien Allonsius, Daniel Song, Danielle Pintz, Danny Livshits, David Esiobu, Dhruv Choudhary, Dhruv Mahajan, Diego Garcia-Olano, Diego Perino, Dieuwke Hupkes, Egor Lakomkin, Ehab AlBadawy, Elina Lobanova, Emily Dinan, Eric Michael Smith, Filip Radenovic, Frank Zhang, Gabriel Synnaeve, Gabrielle Lee, Georgina Lewis Anderson, Graeme Nail, Grégoire Mialon, Guan Pang, Guillem Cucurell, Hailey Nguyen, Hannah Korevaar, Hu Xu, Hugo Touvron, Iliyan Zarov, Imanol Arrieta Ibarra, Isabel M. Kloumann, Ishan Misra, Ivan Evtimov, Jade Copet, Jaewon Lee, Jan Geffert, Jana Vranes, Jason Park, Jay Mahadeokar, Jeet Shah, Jelmer van der Linde, Jennifer Billock, Jenny Hong, Jenya Lee, Jeremy Fu, Jianfeng Chi, Jianyu Huang, Jiawen Liu, Jie Wang, Jiecao Yu, Joanna Bitton, Joe Spisak, Jongsoo Park, Joseph Rocca, Joshua Johnstun, Joshua Saxe, Junteng Jia, Kalyan Vasuden Alwala, Kartikeya Upasani, Kate Plawiak, Ke Li, Kenneth Heafield, Kevin Stone, and et al. 2024. [The llama 3 herd of models](#). *CoRR*, abs/2407.21783.
- Yao Fu. 2024. [Challenges in deploying long-context transformers: A theoretical peak performance analysis](#). *CoRR*, abs/2405.08944.
- Leo Gao, Jonathan Tow, Baber Abbasi, Stella Biderman, Sid Black, Anthony DiPofi, Charles Foster, Laurence Golding, Jeffrey Hsu, Alain Le Noac’h, Haonan Li, Kyle McDonell, Niklas Muennighoff, Chris Ociepa, Jason Phang, Laria Reynolds, Hailey Schoelkopf, Aviya Skowron, Lintang Sutawika, Eric Tang, Anish Thite, Ben Wang, Kevin Wang, and Andy Zou. 2024. [A framework for few-shot language model evaluation](#).
- Xiangyu Hong, Che Jiang, Biqing Qi, Fandong Meng, Mo Yu, Bowen Zhou, and Jie Zhou. 2024. [On the token distance modeling ability of higher RoPE attention dimension](#). In *Findings of the Association for Computational Linguistics: EMNLP 2024*, pages 5877–5888, Miami, Florida, USA. Association for Computational Linguistics.
- Coleman Hooper, Sehoon Kim, Hiva Mohammadzadeh, Michael W. Mahoney, Yakun Sophia Shao, Kurt Keutzer, and Amir Gholami. 2024. [Kvquant: Towards 10 million context length LLM inference with KV cache quantization](#). In *Advances in Neural Information Processing Systems 38: Annual Conference on Neural Information Processing Systems 2024, NeurIPS 2024, Vancouver, BC, Canada, December 10 - 15, 2024*.
- Jingcheng Hu, Houyi Li, Yinmin Zhang, Zili Wang, Shuigeng Zhou, Xiangyu Zhang, and Heung-Yeung Shum. 2024. [Multi-matrix factorization attention](#). *CoRR*, abs/2412.19255.
- Aaron Jaech, Adam Kalai, Adam Lerer, Adam Richardson, Ahmed El-Kishky, Aiden Low, Alec Helyar, Aleksander Madry, Alex Beutel, Alex Carney, Alex Iftimie, Alex Karpenko, Alex Tachard Passos, Alexander Neitz, Alexander Prokofiev, Alexander Wei, Allison Tam, Ally Bennett, Ananya Kumar, Andre Saraiva, Andrea Vallone, Andrew Duberstein, Andrew Kondrich, Andrey Mishchenko, Andy Applebaum, Angela Jiang, Ashvin Nair, Barret Zoph, Behrooz Ghorbani, Ben Rossen, Benjamin Sokolowsky, Boaz Barak, Bob McGrew, Borys Minaiev, Botao Hao, Bowen Baker, Brandon Houghton, Brandon McKinzie, Brydon Eastman,

- Camillo Lugaresi, Cary Bassin, Cary Hudson, Chak Ming Li, Charles de Bourcy, Chelsea Voss, Chen Shen, Chong Zhang, Chris Koch, Chris Orsinger, Christopher Hesse, Claudia Fischer, Clive Chan, Dan Roberts, Daniel Kappler, Daniel Levy, Daniel Selsam, David Dohan, David Farhi, David Mely, David Robinson, Dimitris Tsipras, Doug Li, Dragos Oprica, Eben Freeman, Eddie Zhang, Edmund Wong, Elizabeth Proehl, Enoch Cheung, Eric Mitchell, Eric Wallace, Erik Ritter, Evan Mays, Fan Wang, Felipe Petroski Such, Filippo Raso, Florencia Leoni, Foivos Tsimpourlas, Francis Song, Fred von Lohmann, Freddie Sulit, Geoff Salmon, Giambattista Parascandolo, Gildas Chabot, Grace Zhao, Greg Brockman, Guillaume Leclerc, Hadi Salman, Haiming Bao, Hao Sheng, Hart Andrin, Hessam Bagherinezhad, Hongyu Ren, Hunter Lightman, Hyung Won Chung, Ian Kivlichan, Ian O’Connell, Ian Osband, Ignasi Clavera Gilaberte, and Ilge Akkaya. 2024. [Openai o1 system card](#). *CoRR*, abs/2412.16720.
- Mandar Joshi, Eunsol Choi, Daniel Weld, and Luke Zettlemoyer. 2017. [TriviaQA: A large scale distantly supervised challenge dataset for reading comprehension](#). In *Proceedings of the 55th Annual Meeting of the Association for Computational Linguistics (Volume 1: Long Papers)*, pages 1601–1611, Vancouver, Canada. Association for Computational Linguistics.
- Haoyang Li, Yiming Li, Anxin Tian, Tianhao Tang, Zhanchao Xu, Xuejia Chen, Nicole Hu, Wei Dong, Qing Li, and Lei Chen. 2024. [A survey on large language model acceleration based on KV cache management](#). *CoRR*, abs/2412.19442.
- Zirui Liu, Jiayi Yuan, Hongye Jin, Shaochen Zhong, Zhaozhuo Xu, Vladimir Braverman, Beidi Chen, and Xia Hu. 2024. [KIVI: A tuning-free asymmetric 2bit quantization for KV cache](#). In *Forty-first International Conference on Machine Learning, ICML 2024, Vienna, Austria, July 21-27, 2024*. OpenReview.net.
- Ilya Loshchilov and Frank Hutter. 2019. [Decoupled weight decay regularization](#). In *7th International Conference on Learning Representations, ICLR 2019, New Orleans, LA, USA, May 6-9, 2019*. OpenReview.net.
- Yi Lu, Xin Zhou, Wei He, Jun Zhao, Tao Ji, Tao Gui, Qi Zhang, and Xuanjing Huang. 2024. [LongHeads: Multi-head attention is secretly a long context processor](#). In *Findings of the Association for Computational Linguistics: EMNLP 2024*, pages 7136–7148, Miami, Florida, USA. Association for Computational Linguistics.
- Todor Mihaylov, Peter Clark, Tushar Khot, and Ashish Sabharwal. 2018. [Can a suit of armor conduct electricity? a new dataset for open book question answering](#). In *Proceedings of the 2018 Conference on Empirical Methods in Natural Language Processing*, pages 2381–2391, Brussels, Belgium. Association for Computational Linguistics.
- Guilherme Penedo, Quentin Malartic, Daniel Hesslow, Ruxandra Cojocaru, Hamza Alobeidli, Alessandro Cappelli, Baptiste Pannier, Ebtesam Almazrouei, and Julien Launay. 2023. [The refinedweb dataset for falcon LLM: outperforming curated corpora with web data only](#). In *Advances in Neural Information Processing Systems 36: Annual Conference on Neural Information Processing Systems 2023, NeurIPS 2023, New Orleans, LA, USA, December 10 - 16, 2023*.
- Reiner Pope, Sholto Douglas, Aakanksha Chowdhery, Jacob Devlin, James Bradbury, Jonathan Heek, Kefan Xiao, Shivani Agrawal, and Jeff Dean. 2023. [Efficiently scaling transformer inference](#). In *Proceedings of the Sixth Conference on Machine Learning and Systems, MLSys 2023, Miami, FL, USA, June 4-8, 2023*. mlsys.org.
- Samyam Rajbhandari, Jeff Rasley, Olatunji Ruwase, and Yuxiong He. 2020. [Zero: memory optimizations toward training trillion parameter models](#). In *Proceedings of the International Conference for High Performance Computing, Networking, Storage and Analysis, SC 2020, Virtual Event / Atlanta, Georgia, USA, November 9-19, 2020*, page 20. IEEE/ACM.
- Keisuke Sakaguchi, Ronan Le Bras, Chandra Bhagavatula, and Yejin Choi. 2021. [Winogrande: an adversarial winograd schema challenge at scale](#). *Commun. ACM*, 64(9):99–106.
- Noam Shazeer. 2019. [Fast transformer decoding: One write-head is all you need](#). *CoRR*, abs/1911.02150.
- Jianlin Su, Murtadha H. M. Ahmed, Yu Lu, Shengfeng Pan, Wen Bo, and Yunfeng Liu. 2024. [Roformer: Enhanced transformer with rotary position embedding](#). *Neurocomputing*, 568:127063.
- Hanshi Sun, Li-Wen Chang, Wenlei Bao, Size Zheng, Ningxin Zheng, Xin Liu, Harry Dong, Yuejie Chi, and Beidi Chen. 2024. [Shadowkv: KV cache in shadows for high-throughput long-context LLM inference](#). *CoRR*, abs/2410.21465.
- Hugo Touvron, Louis Martin, Kevin Stone, Peter Albert, Amjad Almahairi, Yasmine Babaei, Nikolay Bashlykov, Soumya Batra, Prajjwal Bhargava, Shrutu Bhosale, Dan Bikel, Lukas Blecher, Cristian Canton-Ferrer, Moya Chen, Guillem Cucurull, David Esiobu, Jude Fernandes, Jeremy Fu, Wenyin Fu, Brian Fuller, Cynthia Gao, Vedanuj Goswami, Naman Goyal, Anthony Hartshorn, Saghar Hosseini, Rui Hou, Hakan Inan, Marcin Kardas, Viktor Kerkez, Madian Khabsa, Isabel Kloumann, Artem Korenev, Punit Singh Koura, Marie-Anne Lachaux, Thibaut Lavril, Jenya Lee, Diana Liskovich, Yinghai Lu, Yuning Mao, Xavier Martinet, Todor Mihaylov, Pushkar Mishra, Igor Molybog, Yixin Nie, Andrew Poulton, Jeremy Reizenstein, Rashi Rungta, Kalyan Saladi, Alan Schelten, Ruan Silva, Eric Michael Smith, Ranjan Subramanian, Xiaoqing Ellen Tan, Binh Tang, Ross Taylor, Adina Williams, Jian Xiang Kuan, Puxin Xu, Zheng Yan, Iliyan Zarov, Yuchen

Zhang, Angela Fan, Melanie Kambadur, Sharan Narang, Aurélien Rodriguez, Robert Stojnic, Sergey Edunov, and Thomas Scialom. 2023. [Llama 2: Open foundation and fine-tuned chat models](#). *CoRR*, abs/2307.09288.

Ashish Vaswani, Noam Shazeer, Niki Parmar, Jakob Uszkoreit, Llion Jones, Aidan N. Gomez, Lukasz Kaiser, and Illia Polosukhin. 2017. [Attention is all you need](#). In *Advances in Neural Information Processing Systems 30: Annual Conference on Neural Information Processing Systems 2017, December 4-9, 2017, Long Beach, CA, USA*, pages 5998–6008.

Xin Wang, Yu Zheng, Zhongwei Wan, and Mi Zhang. 2025. [SVD-LLM: Truncation-aware singular value decomposition for large language model compression](#). In *The Thirteenth International Conference on Learning Representations*.

An Yang, Baosong Yang, Beichen Zhang, Binyuan Hui, Bo Zheng, Bowen Yu, Chengyuan Li, Dayiheng Liu, Fei Huang, Haoran Wei, Huan Lin, Jian Yang, Jianhong Tu, Jianwei Zhang, Jianxin Yang, Jiayi Yang, Jingren Zhou, Junyang Lin, Kai Dang, Keming Lu, Keqin Bao, Kexin Yang, Le Yu, Mei Li, Mingfeng Xue, Pei Zhang, Qin Zhu, Rui Men, Runji Lin, Tianhao Li, Tingyu Xia, Xingzhang Ren, Xuancheng Ren, Yang Fan, Yang Su, Yichang Zhang, Yu Wan, Yuqiong Liu, Zeyu Cui, Zhenru Zhang, and Zihan Qiu. 2024. [Qwen2.5 technical report](#). *CoRR*, abs/2412.15115.

Rowan Zellers, Ari Holtzman, Yonatan Bisk, Ali Farhadi, and Yejin Choi. 2019. [HellaSwag: Can a machine really finish your sentence?](#) In *Proceedings of the 57th Annual Meeting of the Association for Computational Linguistics*, pages 4791–4800, Florence, Italy. Association for Computational Linguistics.

Boyang Zhang, Daning Cheng, Yunquan Zhang, Fangmin Liu, and Jiake Tian. 2024a. [Lossless model compression via joint low-rank factorization optimization](#). *CoRR*, abs/2412.06867.

Rongzhi Zhang, Kuang Wang, Liyuan Liu, Shuohang Wang, Hao Cheng, Chao Zhang, and Yelong Shen. 2024b. [Lorc: Low-rank compression for llms KV cache with a progressive compression strategy](#). *CoRR*, abs/2410.03111.

Yilong Zhao, Chien-Yu Lin, Kan Zhu, Zihao Ye, Lequn Chen, Size Zheng, Luis Ceze, Arvind Krishnamurthy, Tianqi Chen, and Baris Kasikci. 2024. [Atom: Low-bit quantization for efficient and accurate LLM serving](#). In *Proceedings of the Seventh Annual Conference on Machine Learning and Systems, MLSys 2024, Santa Clara, CA, USA, May 13-16, 2024*. mlsys.org.

A More Detail on the Preference Pattern of Each Attentional Head

For a more detailed frequency preference pattern, refer to Figure 8.

B Analysis of RoPElite Time Consumption

We analyze the time complexity of RoPElite. Our method computes the top- r chunks for each layer and head with a time complexity of $O(rh_d)$ forward pass. To obtain the top- r chunks, the algorithm requires r iterations. In each iteration, the influence of each chunk in \mathcal{I}_r^e on the attention scores is computed, and the chunk that most closely approximates the original RoPE attention scores is selected and added to \mathcal{I}_r^e .

In practice, the computation for different heads is parallelized. Although the top- r selection differs across heads, the calculations of attention score are independent for each head. This allows us to leverage the parallelism of matrix operations, computing the influence of a given chunk on attention scores for all heads in a single forward pass.

Calculations for different layers can also be performed simultaneously within the same forward pass. During the computation, we only calculate the attention scores of applying RoPE on specific chunks within the attention block, while using the attention scores of the original RoPE during the forward pass. This approach ensures the independence of the algorithm across different layers.

C Dimension Allocation of RoPElite and LRD

For a given KV cache size, there exist numerous valid dimension configurations for both *RoPElite* and the LRD components. This introduces an optimization challenge, as selecting the appropriate dimensions of *RoPElite* and LRD to achieve the optimal performance requires balancing the contributions of both components under the constraint of a fixed total size. To simplify this allocation problem, we adopt the following strategies.

Hardware-Friendly. For optimal hardware compatibility, the primary design principle is to ensure that the intermediate dimension of LRD, c_{kv} , is aligned with multiples of 128 across all valid configurations.³

No Additional Parameters. Since low rank decomposition may lead to an increase in the number of parameters, a fair approach to prevent

³For further details on the requirements and performance considerations of Tensor Cores, refer to [NVIDIA’s official documentation](#).

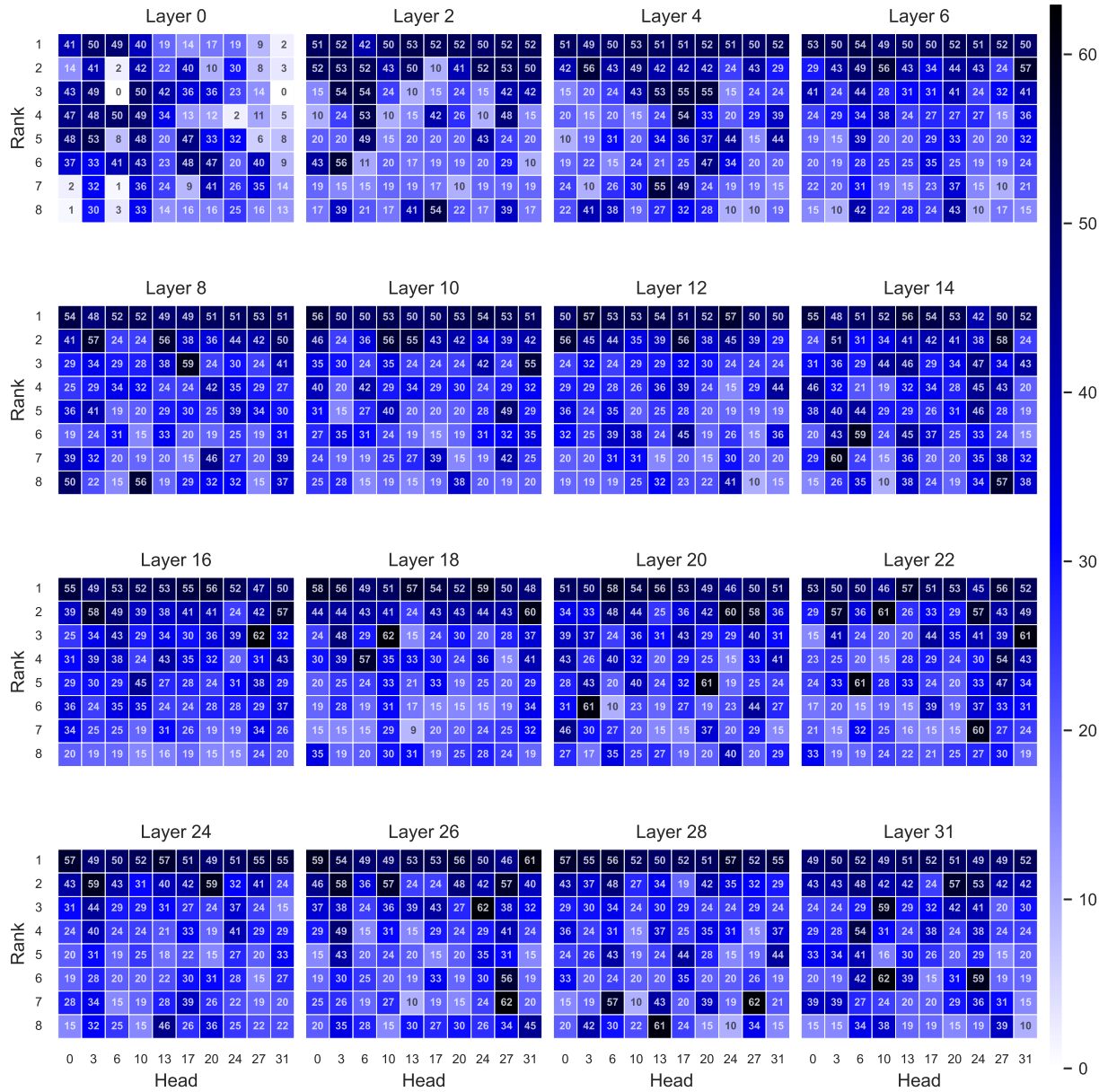


Figure 8: Top- r chunks of different attention heads in different layers.

sacrificing parameter efficiency for a smaller KV cache is to ensure that the total number of parameters does not increase after applying low rank decomposition.

Lower Perplexity. Under these two constraints, a set of potential dimension configurations is selected. These configurations are then evaluated based on language perplexity on a holdout dataset, and those with lower perplexity are chosen as the final dimension design for a given KV cache.